

# Inhibition of Proliferation, Invasion, and Migration of Prostate Cancer Cells by Downregulating Elongation Factor-1 $\alpha$ Expression

Gang Zhu,<sup>1\*</sup> Wei Yan,<sup>1\*</sup> Hui-chan He,<sup>2\*</sup> Xue-cheng Bi,<sup>2</sup> Zhao-dong Han,<sup>2</sup> Qi-shan Dai,<sup>2</sup> Yong-kang Ye,<sup>2</sup> Yu-xiang Liang,<sup>2</sup> Jianye Wang,<sup>1</sup> and Weide Zhong<sup>2</sup>

<sup>1</sup>Department of Urology, Beijing Hospital MH, Beijing, China; <sup>2</sup>Guangzhou First Municipal People's Hospital, Affiliated Guangzhou Medical College, Guangzhou, China

Overexpression of elongation factor-1 $\alpha$  (EF-1 $\alpha$ ) has been reported to contribute to the development and progression of various cancers. However, its role in prostate cancer (PCa) still remains poorly understood. In the present study, we investigate the influence of EF-1 $\alpha$  in Du145, a high-grade metastatic PCa cell line, and demonstrate that EF-1 $\alpha$  plays an essential role in cellular properties associated with tumor progression, namely cell proliferation, invasion, and migration. In this study, EF-1 $\alpha$  expression in human PCa cell line Du145 was reduced by RNA interference (RNAi) technology, and the proliferation, invasion, and migration of EF-1 $\alpha$ -reduced Du145 cells were examined. We also detected an EF-1 $\alpha$  expression pattern in 20 pairs of primary PCa samples and their corresponding normal tissues. Expression of EF-1 $\alpha$  was detectable in four PCa cell lines (22RV1, LnCap, Du145, and PC3), indicating its possible role in pathogenesis of PCa. RNAi-mediated knockdown of EF-1 $\alpha$  expression in Du145 cells, which expressed the highest level of EF-1 $\alpha$  among four PCa cell lines, led to a decrease in proliferation. Similarly, suppression of EF-1 $\alpha$  inhibited Du145 cell migration and invasion through a basement membrane substitute. Furthermore, we found that the normal prostate tissues showed a relatively low level of EF-1 $\alpha$  expression, whereas PCa tissues demonstrated significantly higher expression levels of EF-1 $\alpha$  ( $P < 0.001$ ). Taken together, these findings support the hypothesis that EF-1 $\alpha$  affects multiple processes involved in tumor progression, and identify EF-1 $\alpha$  as a potential therapeutic target.

© 2009 The Feinstein Institute for Medical Research, [www.feinsteininstitute.org](http://www.feinsteininstitute.org)

Online address: <http://www.molmed.org>

doi: 10.2119/molmed.2009.00082

## INTRODUCTION

Prostate cancer (PCa) poses a major public health problem worldwide. Diagnosis and treatment of PCa has had many advances in the past 20 years; unfortunately, the existing treatment approaches and surgical interventions have been proven to be inadequate for the management of this disease (1,2). PCa deaths are a result of metastatic disease and treatment of such metastatic disease is one of the major therapeutic challenges. Thus, there is a need to develop novel thera-

peutic approaches and strategies. Many studies have focused on identification of the molecular mechanisms of development and progression of PCa, which are complicated and likely to involve multiple factors, such as tumor suppressor genes, oncogenes, growth factors, adhesion molecules, and angiogenesis (3–6). PCa cells with high- and low-metastatic potential vary in their biological properties, such as proliferation, adhesiveness, invasiveness, and motility. Differences in gene expression between normal cells

and PCa cells often provide interesting targets for anti-neoplastic therapy. For this reason, considerable efforts have been made to understand the genetic controls of cellular proliferation and cell division clearly, which may provide the basis for the rational design of therapeutic strategies for the management of PCa.

Elongation factor-1 $\alpha$  (EF-1 $\alpha$ ) has been reported as an actin binding protein in many divergent species, such as carrot, tetrahymena, rabbit, and mouse (7). The intracellular distribution of EF-1 $\alpha$  has been demonstrated to co-localize with filamentous actin (F-actin), and also is correlated with changes in the organization of the actin cytoskeleton during chemotaxis (8). It has been reported that there is a high degree of amino acid sequence conservation across phylogeny, and actin binding activity is a universal property of all EF-1 $\alpha$  (9). The control of EF-1 $\alpha$  levels is important for normal cell

---

\*GZ, WY, and HH contributed equally to this paper.

**Address correspondence and reprint requests to** Weide Zhong, First Municipal People's Hospital, Affiliated Guangzhou Medical College, Guangzhou 510180, China. Phone: +86-0-13808888068; Fax: +86-20-83373322; E-mail: [wdezhong@21cn.com](mailto:wdezhong@21cn.com); or Jianye Wang, Department of Urology, Beijing Hospital MH, Beijing 100730, China. Phone: +86-1085136806; Fax: +86-1065132969; E-mail: [wangjy@bjhmoh.cn](mailto:wangjy@bjhmoh.cn).

Submitted June 24, 2009; Accepted for publication August 14, 2009; Epub ([www.molmed.org](http://www.molmed.org)) ahead of print August 18, 2009.

function. EF-1 $\alpha$  has been shown to be an important regulator of the cell cycle and is overexpressed in tumors of the pancreas, colon, breast, lung, and stomach compared with levels in normal tissue (10). In addition, overexpression of EF-1 $\alpha$  mRNA was correlated with metastasis. However, its role in PCa still remains poorly understood. To address this problem, in the present study, we investigated the influence of EF-1 $\alpha$  in Du145, a high-grade metastatic PCa cell line, and demonstrated that EF-1 $\alpha$  played an essential role in cellular properties associated with tumor progression, namely cell proliferation, invasion, and migration.

## MATERIALS AND METHODS

### PCa Tissue Samples and Cell Lines

Our study was approved by the Ethics Committee of Beijing Hospital of China; 20 pairs of primary PCa samples and their corresponding normal tissues were obtained from PCa patients treated at Beijing Hospital of China from 2006 to 2008 after their written informed consent. All of the tissues were obtained immediately during the operation of transurethral resection prostate and suprapubic radical prostatectomy. Surgically resected tissues were paraffin-embedded, sectioned at 3-mm thickness, and used for immunohistochemical staining. The pathological diagnosis of prostate biopsy was performed preoperatively and confirmed postoperatively.

Four PCa cell lines (22RV1, LnCap, Du145, and PC3) were purchased from the Cell Center of Institute of Basic Medical Sciences in Chinese Academy of Medical Sciences (Beijing, China) and cultured in RPMI-1640 (GIBCO, Langley, OK, USA), supplemented with 10% fetal bovine serum (GIBCO), 10U/mL penicillin, and 10U/mL streptomycin, at 37°C in a humidified atmosphere containing 5% CO<sub>2</sub>. 22RV1 and LnCap are androgen sensitive cell lines derived from a PCa lymph node metastasis, whereas Du145 and PC3 are androgen insensitive cell lines derived from PCa bone metastases.

### Quantitative Real-Time Polymerase Chain Reaction (QRT-PCR)

Total RNA of four PCa cell lines (22RV1, LnCap, Du145, and PC3) were prepared, reverse transcribed, and QRT-PCR carried out as described previously (11). The primers 5'-AAC ATC GTC GTG ATH GGN CAY GTN GA-3' and 5'-CTT GAT CAC NCC NAC NGC NAC NGT-3' were used to amplify 450-bp transcripts of EF-1 $\alpha$ , and the primers 5'-GTG CCA CCA GAC AGC ACT GTG TTG-3' and 5'-TGG AGA AGA GCT ATG AGC TGC CTG-3' were used to amplify 202-bp transcripts of  $\beta$ -actin. Product-specific amplification was confirmed by melting curve analysis and agarose gel electrophoresis. Serial dilutions were made using previously generated PCR products, assigned arbitrary values corresponding to the dilutions, and used to construct relative standard curves for EF-1 $\alpha$ . Targets were normalized using  $\beta$ -actin as an internal standard.

### Small Interfering RNA (siRNA) Synthesis and Transient Transfection

Sense and antisense RNAs corresponding to the EF-1 $\alpha$  cDNA sequence (AUG CGG UGG CAU CGA CAA A from BC001412; National Center for Biotechnology Information, GenBank, Bethesda, MD, USA) and the nonspecific control siRNA (CCU CCA AUC UUC GCG CGU C) (siRNA-C) were chemically synthesized, annealed (siRNA-E) and purchased from Dharmacon Research Inc. (Lafayette, CO, USA).

Twenty-four h before transfection, 3 $\times$ 10<sup>5</sup> Du145 cells were seeded into a T25 flask in 5 mL OPTI-MEM medium with 10% fetal bovine serum. Oligofectamine Kit (Invitrogen, Carlsbad, CA, USA) was used to transfect siRNAs into cells according to the procedures recommended by the manufacturer. An amount of 1 nmol siRNA was used for each T25 flask. In cases of apparent overconfluence, assessed by simple visual examination, cells were split on the second d after the transfection, but the cells were maintained in various media containing the siRNA at the appropriate concentration.

All assays were carried out on d 3 after transfection, except the Western blotting and the growth curve study, which was initiated on d 1 after the transfection and continued over the subsequent 6 d.

### Western Blot Analysis

Du145 cells in nontransfected group, siRNA-C-transfected group, and siRNA-E-transfected group were cultured in complete growth media to 70% confluence, then replaced with serum-free RPMI-1640 and incubated for 48 h. The suspensions of Du145 cells in three groups were centrifuged (71.55g) and the cell pellets were washed with ice-cold PBS. Total proteins were extracted with lysis buffer (150 mmol/L NaCl, 50 mmol/L Tris-HCl, pH 7.4, 2 mmol/L EDTA, 1% NP-40) containing protease inhibitors. The protein content was determined according to Bradford's method (12), with bovine serum albumin used as a standard. Protein samples (30  $\mu$ g) were boiled with 2 $\times$  sample buffer containing 5%  $\beta$ -mercaptoethanol for 5 min, separated by size on 15% polyacrylamide gel under SDS denaturing conditions, and transferred to a nitrocellulose membrane at 90 V for 2 h. The nitrocellulose membranes were stained with ponceau S to assess the efficiency of transfer. Nonspecific binding was blocked by incubation in block buffer (5% nonfat dry milk, 0.05% Tween-20, 1 $\times$  Tris-Cl-buffered saline, Rockland Immunochemicals Inc., Gilbertsville, PA, USA) overnight at 4°C. The membranes were hybridized with a mouse anti-human EF-1 $\alpha$  monoclonal antibody (at the dilution of 1:500, Upstate Biotechnology, Lake Placid, NY, USA) and mouse anti-human  $\beta$ -actin monoclonal antibody (at the dilution of 1:1000, Santa Cruz Biotechnology, Santa Cruz, CA, USA), then incubated with a horseradish peroxidase-labeled goat anti-rabbit IgG (1:500). The bound secondary antibody was detected by enhanced chemiluminescence (Amersham Life Science, Little Chalfont, UK). Housekeeping protein  $\beta$ -actin was used as a loading control. Positive immunoreactive bands were quantified densitometrically (Leica

Q500IW image analysis system, Leica Cambridge Ltd., Cambridge, UK) and expressed as ratio of EF-1 $\alpha$  to  $\beta$ -actin in optical density units, respectively.

### Immunofluorescence

For the immunofluorescence detection of EF-1 $\alpha$  and F-actin, Du145 cells of nontransfected group, siRNA-C–transfected group, and siRNA-E–transfected group were seeded (40,000 cells/22-x-22-mm glass coverslips in 3-cm-diameter Petri dishes) and treated according to the standard protocol described previously (13). The cultures were fixed in cold methanol and then immunoreacted with the primary antibodies (polyclonal antibodies anti-human EF-1 $\alpha$  at a dilution of 1:50 [Upstate Biotechnology] and anti-F-actin antibodies at a dilution of 1:50 [Santa Cruz Biotechnology]). The cells then were immunoreacted with the secondary antibodies fluorescein-conjugated anti-rabbit IgG (at a dilution of 1:50, Calbiochem, San Diego, CA, USA) and rhodamine-conjugated anti-mouse IgG (at a dilution of 1:50, Calbiochem). The coverslips were mounted on glass slides in mounting medium and photographed with an Olympus fluorescence microscope (Olympus Optical Company Ltd., Tokyo, Japan). Ten randomly chosen fields were analyzed for each cell type with a specific analysis system (IAS) program to evaluate the integrated optical density level of each immunofluorescent cell.

### Proliferation Assays

To determine proliferation,  $1 \times 10^4$  Du145 cells of nontransfected group, siRNA-C–transfected group, and siRNA-E–transfected group were plated in triplicates in 6-well culture plates. On each sixth consecutive d, one plate was removed, and 0.1 vol of MTT Solution (3-[4,5-dimethylthiazolyl-2]-2,5-diphenyl tetrazolium bromide; MP Biomedicals Inc, Solon, OH, USA) was added to each well and incubated for 4 h at 37°C. After removal of all supernatant, 1 mL of MTT solubilization solution (10% SDS in 0.01 M HCl) was added and incubated overnight at 37°C.

After all crystals were solubilized, the optical density of the solution was determined spectrophotometrically at 570 nm. Alternatively, cells were plated in triplicate wells, as described above, then trypsinized daily, and counted using a hemocytometer.

### Migration and Invasion Assays

Du145 cells of nontransfected group, siRNA-C–transfected group, and siRNA-E–transfected group at 70% confluence were detached from culture plates in the absence of trypsin using Hank's buffered saline solution (HBSS)/5 mM EDTA/25 mM Hepes pH 7.2 (Mediatech, Herndon, VA, USA). Cells then were washed twice in RPMI-1640/0.1% BSA and resuspended at a density of  $2.5 \times 10^5$ /mL in RPMI-1640/0.1% BSA; 200  $\mu$ l of the cell suspension was added to the upper chamber of an 8  $\mu$ m pore size Transwell insert (Becton Dickinson, Becton Drive, Franklin Lakes, NJ, USA) in triplicate. Serum-free RPMI-1640/0.1% BSA containing 10 ng/mL EGF was added to the lower chamber of each well and incubated for 20 h at 37°C. Cells were fixed with 0.025% glutaraldehyde (Sigma Aldrich, St. Louis, MO, USA) in PBS, stained in 0.1% crystal violet, and nonmigratory cells on the upper surface of the membrane removed. Membranes were mounted on a microscope slide, and migrated cells were counted in five random high-power fields.

Invasion assays were carried out in a similar manner to migration assays. Transwell inserts with 12- $\mu$ m pores (Becton Dickinson) were coated with 200  $\mu$ l Matrigel (Becton Dickinson), which was diluted 1:6 in ice-cold RPMI-1640, and allowed to gel at 37°C. Subconfluent cell cultures were detached as described above, resuspended in RPMI-1640/0.1% BSA, and  $5 \times 10^4$  cells seeded in the upper chamber. Culture plates were incubated for 16 h at 37°C, and the cells fixed, stained, and counted as described above.

### Immunohistochemistry Analysis

The specimens were fixed in 10% neutral buffered formalin and subsequently

embedded in paraffin. The paraffin-embedded tissues were cut at 3  $\mu$ m, and then deparaffinized with xylene, and rehydrated for further hematoxylin and eosin (H&E) or peroxidase (DAB) immunohistochemistry staining employing DAKO EnVision System (Dako Diagnostics, Zug, Switzerland). Following a brief proteolytic digestion and a peroxidase blocking of tissue slides, the slides were incubated overnight with the primary antibody against EF-1 $\alpha$  (Upstate Biotechnology) at a dilution of 1:100 at 4°C. After washing, peroxidase-labeled polymer and substrate-chromogen were employed to visualize the staining of the interested proteins. Normal prostate tissues were used as control for immunohistochemical staining.

Following a hematoxylin counterstaining, immunostaining was scored by three independent, experienced pathologists, who were blinded to the clinicopathological data and clinical outcomes of the patients. The scores of the three pathologists were compared and any discrepant scores were trained through reexamining the stainings by both pathologists to achieve a consensus score. The number of positive-staining cells showing immunoreactivity on the cytoplasm in ten representative microscopic fields was counted and the percentage of positive cells was calculated. Given the homogeneity of the staining of the target proteins, tumor specimens were scored in a semiquantitative manner based on the percentage of tumor cells that showed immunoreactivity. The criteria used for the assessment of EF-1 $\alpha$  expression was 0 (negative or weak,  $\leq 5\%$ ), 1+ (moderate,  $\sim 5\% \sim 50\%$ ), and 2+ (intensive,  $> 50\%$ ) of the tumor cells stained.

### Statistical Analysis

The software of SPSS version 13.0 for Windows (SPSS Inc, Chicago, IL, USA) was used for statistical analysis. Continuous variables were expressed as  $\bar{X} \pm s$ . Statistical analysis was performed with *t*-test. Differences were considered statistically significant when *P* was less than 0.05.

RESULTS

EF-1 $\alpha$  Expression Varies in PCa Cells

QRT-PCR was performed to determine if EF-1 $\alpha$  expression was elevated in PCa cell lines (22RV1, LnCap, Du145, and PC3). As shown in Figure 1, the two highly malignant cell lines (PC3 and Du145), indeed, exhibited significantly higher EF-1 $\alpha$  expression than that in the other two less malignant cell lines (22RV1 and LnCap) ( $P = 0.009$  for Du145 versus 22RV1;  $P = 0.01$  for PC3 versus 22RV1;  $P = 0.01$  for Du145 versus LnCap;  $P = 0.02$  for PC3 versus LnCap;  $P > 0.05$  for 22RV1 versus LnCap and Du145 versus PC3). Especially, Du145 expressed the highest level of EF-1 $\alpha$ . As Du145 cells were derived from PCa bone metastases and exhibit distinct proliferative and motile properties, we selected these for further study.

Confirmation of siRNA-Mediated Downregulation of EF-1 $\alpha$  Gene by Western Blotting and Immunofluorescence Analysis

To determine whether the expression of siRNA-E affected EF-1 $\alpha$  protein production, Du145 cells of nontransfected group, siRNA-C-transfected group, and siRNA-E-transfected group were used to perform Western blotting analysis with monoclonal anti-human EF-1 $\alpha$  antibody. A specific 56kDa protein band was present in all the samples of nontransfected group and siRNA-C-transfected group without any change during 6 d, while the expression of EF-1 $\alpha$  in the samples of siRNA-E-transfected group was reduced constantly from d 1 to d 6 after the transfection (Figure 2A). Furthermore, densitometric analysis of the Western blotting also showed a significant decrease in the amount of EF-1 $\alpha$  from siRNA-E-transfected cells in a time-dependent manner, while there were no changes with statistical significance in nontransfected cells and siRNA-C-transfected cells (Figure 2B).

Similarly, the immunofluorescence analysis with monoclonal anti-EF-1 $\alpha$  and monoclonal anti-F-actin antibodies also showed that EF-1 $\alpha$  fluorescent protein

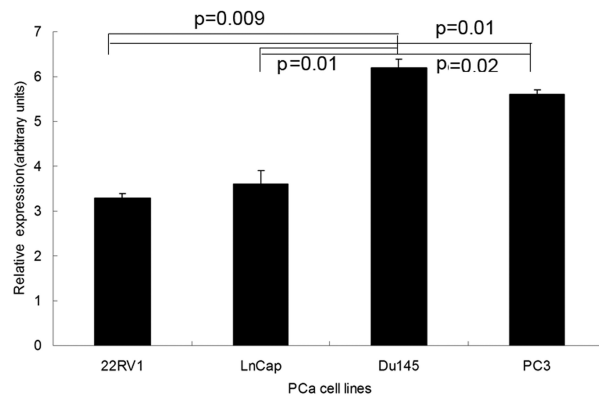


Figure 1. EF-1 $\alpha$  expression in PCa cell lines 22RV1, LnCap, Du145, and PC3. Total RNA was prepared from the indicated cell lines, reverse-transcribed, and subjected to QRT-PCR using oligonucleotide primers specific for EF-1 $\pm\alpha$ . Expression was normalized using  $\beta$ -actin expression as an internal standard.

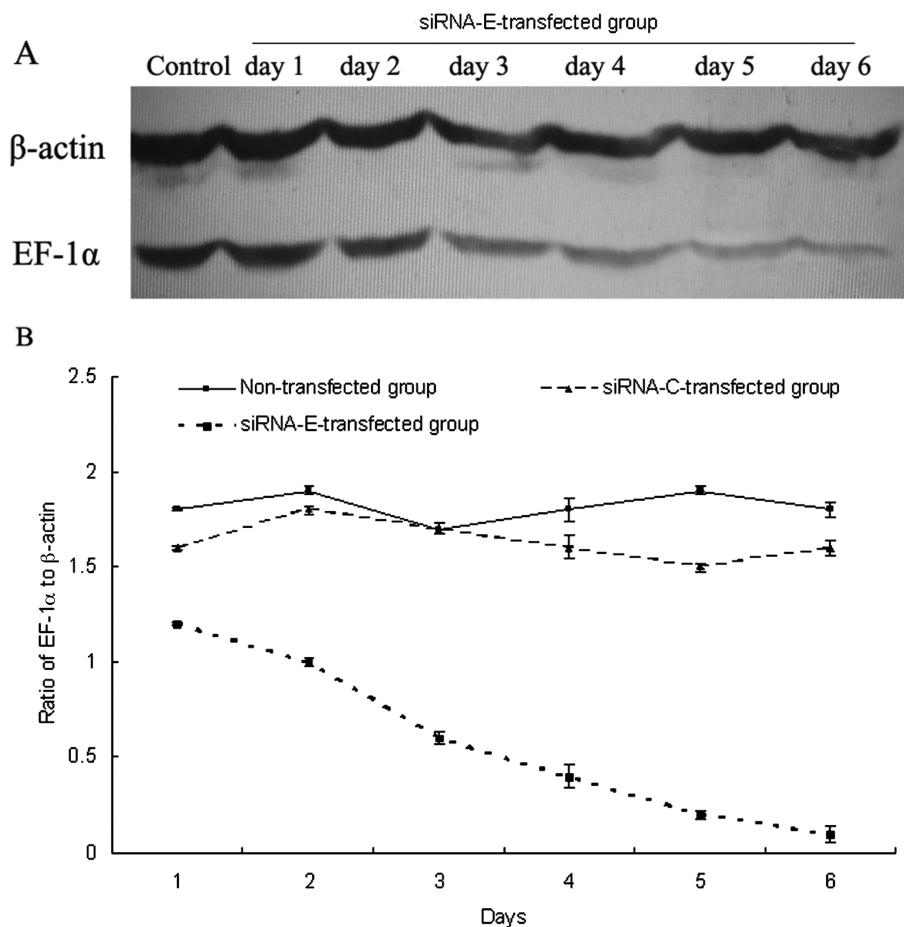
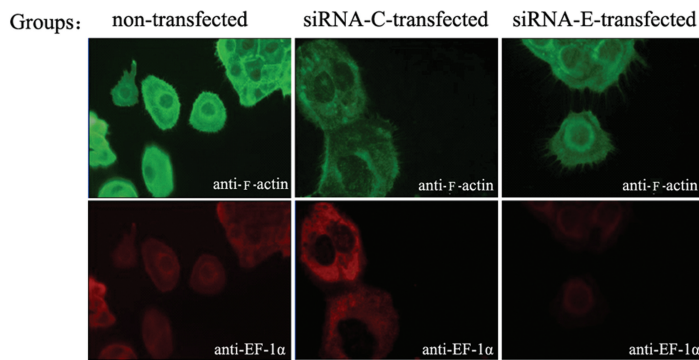


Figure 2. Stable suppression of EF-1 $\alpha$  by siRNA in Du145 cells. (A) Du145 cells were transfected with either siRNA-C or siRNA-E. Cells were then lysed and subjected to Western blot analysis with either anti-EF-1 $\alpha$  or anti- $\beta$ -actin antibodies. (B) Densitometric analysis of EF-1 $\alpha$  protein in cells of nontransfected group, siRNA-C-transfected group, and siRNA-E-transfected group.



**Figure 3.** Du145 cells were cultured in 6-well chamber slides at a concentration of  $1 \times 10^4$  and transfected with either siRNA-C or siRNA-E; parental cells were simultaneously maintained; 72 h after transfection, the cells were fixed in cold methanol. Expression of EF-1 $\alpha$  was detected in intact cells (see Materials and Methods).

signal of Du145 cells in siRNA-E-transfected group was reduced distinctly at d 3 after the transfection, compared with that of nontransfected group and siRNA-C-transfected group (Figure 3). In addition, EF-1 $\alpha$  immunofluorescent signal was colocalized with F-actin, which

was similar in nontransfected and transfected cells (see Figure 3).

#### Effect of EF-1 $\alpha$ Downregulation on Proliferation of Du145 Cells

To better understand the role that EF1 $\alpha$  plays in tumor progression, we

determined the proliferation rates of Du145 cells in different groups. As shown in Figure 4A, Du145 cells expressing EF-1 $\alpha$  siRNA exhibited a decreased rate of growth compared with nontransfected and siRNA-C-transfected cells as judged by MTT assay ( $P = 0.02$  for siRNA-E transfected group versus nontransfected group;  $P = 0.03$  for siRNA-E-transfected group versus siRNA-C-transfected group). Similar results were obtained in cell counting assays (Figure 4B). Taken together, these data indicated that EF-1 $\alpha$  potentiated Du145 cell proliferation.

#### Effect of EF-1 $\alpha$ Downregulation on Migration and Invasion of Du145 Cells

To test whether EF-1 $\alpha$  expression affects motility of our model cell line (Du145), we carried out standard *in vitro* chamber assays. As shown in Figure 5A, migration of Du145 cells was repressed 3.56-fold and 3.64-fold by EF-1 $\alpha$  siRNA-mediated suppression compared with nontransfected and siRNA-C-transfected cells. To extend our studies, we assayed the capacity of cells expressing EF-1 $\alpha$  siRNA to invade through Matrigel-coated Transwell inserts. Consistent with the results of migration assays, repression of EF-1 $\alpha$  expression in Du145 cells was found to inhibit *in vitro* invasion (Figure 5B). Taken together, these data indicated that EF-1 $\alpha$  enhanced motility and invasion of Du145 cells.

#### 3.5 EF-1 $\alpha$ Expression Pattern Was Associated with PCa Progression

The immunohistochemical staining was performed to detect the EF-1 $\alpha$  expression pattern in the region of cancerous tissues and their matched normal prostate tissues. A representative figure showed that the expression of EF-1 $\alpha$  was mild in both gland cells and stromal smooth muscle cells in normal prostate tissues, whereas higher level of EF-1 $\alpha$  expression was observed in epithelial PCa foci and the stromal smooth muscle cells in tumor samples (Figure 6). Consistent with these results, the positive expression rate of EF-1 $\alpha$  in PCa tissues was

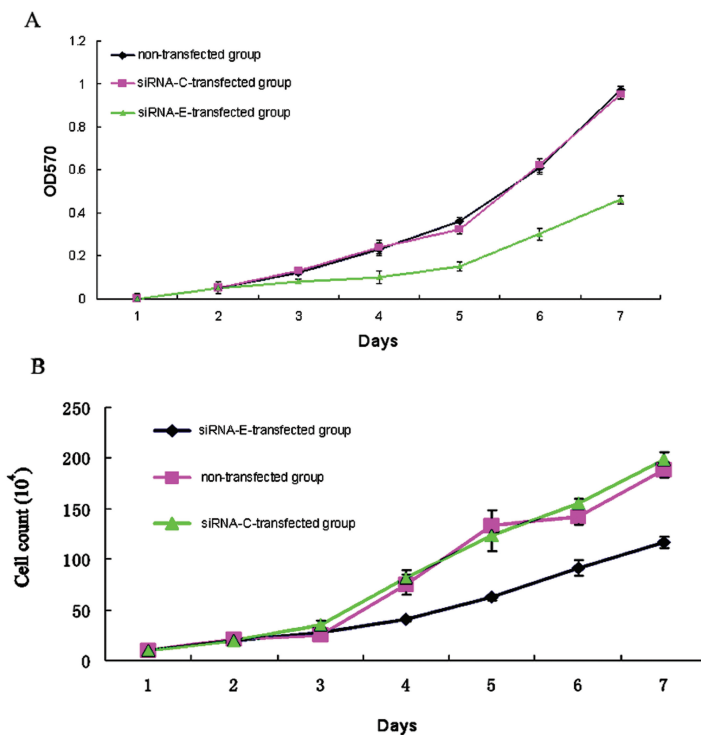


**Figure 4.** EF-1 $\alpha$  enhances proliferation of Du145 cells. Equal numbers of indicated cells were plated in triplicate, incubated under standard culture conditions, following the MTT assays (A) and the cell counting assay (B) as described in Materials and Methods. Values shown are  $\bar{X} \pm s$ .

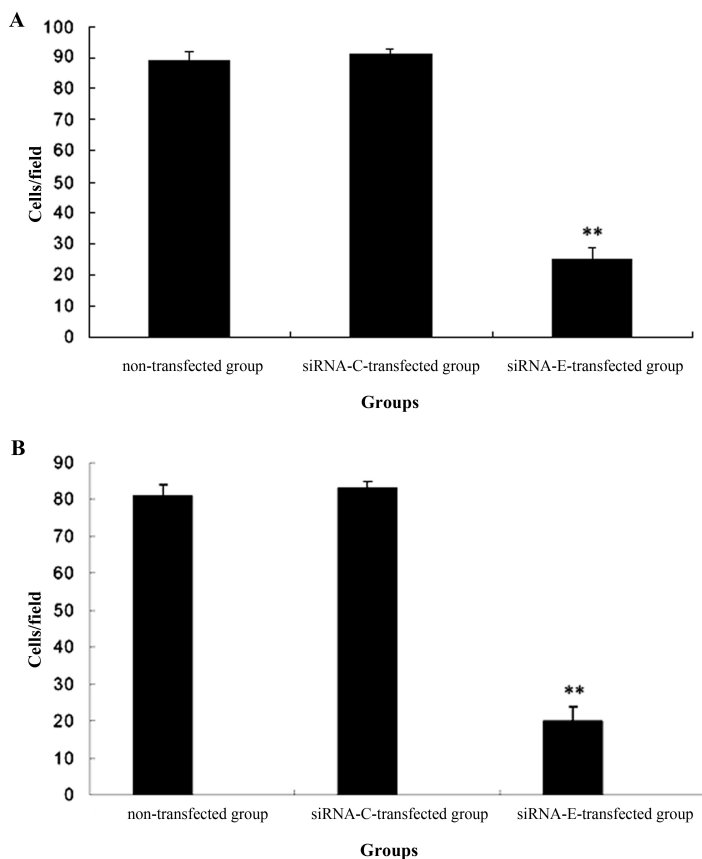


**Figure 5.** EF-1 $\alpha$  is important for migration and invasion of Du145 cells. (A) The indicated cells were detached from culture plates, washed, and plated in the upper chamber of Transwell inserts as described in Materials and Methods. After 20 h, migrated cells were stained and counted in five random high power fields. (B) The indicated cells were plated in Matrigel-coated Transwell chambers as described in Materials and Methods; 16 h later, invading cells were stained and counted in five random high power fields. Values shown are  $\bar{X} \pm s$ . \*\* $P < 0.001$ , comparison of the number of siRNA-E-transfected Du145 cells/field with that of nontransfected and siRNA-C-transfected Du145 cells/field.

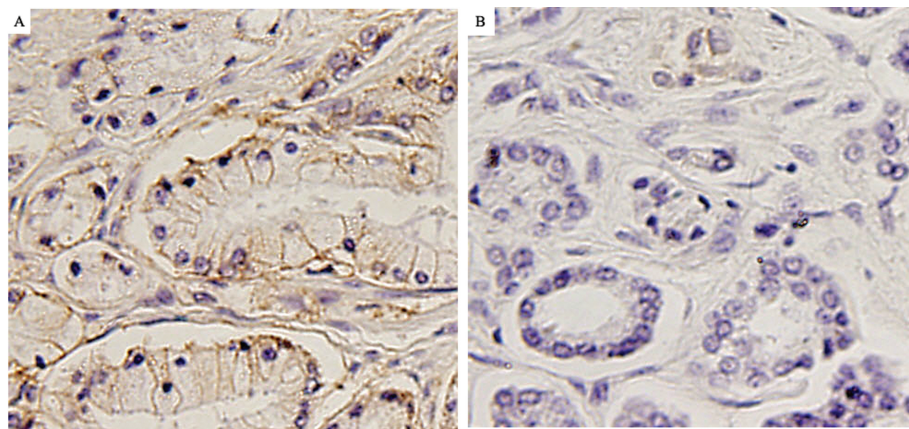


**Figure 6.** Immunohistochemical staining of EF-1 $\alpha$  in clinical PCa tissues (A) and matched normal prostate tissue (B) (400 $\times$ ).

80% (16/20), which was significantly higher than the 20% (4/20) ( $P < 0.001$ ) in normal prostate tissues. Taken together, these data indicated that EF-1 $\alpha$  played a stimulative role in the tumorigenesis of PCa and prompted the metastasis of malignant PCa cells.

## DISCUSSION

The present study explored whether RNAi-mediated suppression of EF-1 $\alpha$  could be used to inhibit the proliferative and motile characteristics of PCa cells, and demonstrated that EF-1 $\alpha$  regulated tumor cell growth, invasion, and migration, suggesting that EF-1 $\alpha$  might act as an oncoprotein in PCa.

Metastasis of a malignant tumor is the leading cause of death. However, the molecular mechanisms underlying the migration of cells from the primary tumor to ectopic sites are unclear. Some researchers have argued that the metastatic process is similar to the chemotaxis of motile cells along gradients of cytokines (14–16). In this regard, it is likely that molecules identified as important for mounting the chemotactic response also may be important for metastasis. The principal effector of the chemotactic response is the cellular motile machinery composed of the actin cytoskeleton (17). Polarized surface projections containing newly polymerized actin are formed in response to intracellular signaling molecules generated by the binding of cytokines to their membrane-bound receptors (18). The stabilization of these actin-containing projections by various families of actin binding proteins allows the cell to move in the specific direction of the cytokine gradient. One such family of actin binding proteins consists of those proteins that crosslink actin filaments into bundled arrays (19). EF-1 $\alpha$ , an abundant member of the actin bundling protein family, is the cofactor of eukaryotic protein synthesis responsible for binding aminoacyl-tRNA to the ribosome during polypeptide elongation (20–21). EF-1 $\alpha$  not only functions as a polypeptide elongation factor, an activity that might indicate the greater

metabolic activity of peripheral tumor cells, but also is a well-characterized F-actin and microtubule-binding protein (22). Interestingly, the overexpression of EF-1 $\alpha$  already has been correlated with increased metastatic propensity (23).

In our study, we found that EF-1 $\alpha$  immunofluorescent signal was co-localized with F-actin, which has been reported previously (24). We also demonstrated that the knockdown of EF-1 $\alpha$  resulted in the decrease of growth in Du145 cells, which was consistent with the inhibition of migration and invasion. Mohler *et al.* (25) has already shown that EF-1 $\alpha$  was 1 of 11 candidate genes which triggered the tumor proliferation of recurrent CWR22, an androgen-dependent xenograft model derived from a primary human PCa. So the effect of EF-1 $\alpha$  in regulation of PCa mechanisms in androgen sensitive cells lines should be increasing proliferation. Furthermore, the higher positive expression rate of EF-1 $\alpha$  in clinical PCa samples than their matched normal prostate tissues make us speculate that EF-1 $\alpha$  might play distinct roles in PCa with different degrees of malignance; however, this hypothesis required further investigations.

As already stated, RNAi technology uses an intricate natural pathway for sequence-specific mRNA degradation and regulates gene expression at the post-transcriptional level (26). Delivery of small RNA is accomplished through several methods. While synthetic RNA duplexes are introduced into biological systems directly, the RNAi effect is only transient (27). However, recent studies indicate that introducing DNA-directed RNAi expression cassettes through plasmid or viral vectors serve as an excellent source of RNAi supply to the biological system under investigation (28–29). In this case, dsRNA is expressed continuously within the cells using the DNA templates that direct synthesis of RNA duplexes or short hairpin RNAs, and thus, depending on the vector employed, RNAi effect can be sustained long term (30). The size of the siRNA molecules is small enough to be

transmitted from cell to cell, which has been reported previously (31). Inhibiting the expression of pathogenic genes by siRNA-induced RNAi has proved to be a successful approach to reducing the malignance of different tumor cells (32). In this study, we selectively reduced EF-1 $\alpha$  expression in human PCa cells by exploiting RNAi technology. Furthermore, selective inhibition of EF-1 $\alpha$  significantly reduced metastatic potential of EF-1 $\alpha$ -expressing human PCa cell *in vitro* by affecting multiple aspects of tumor invasion.

In summary, EF-1 $\alpha$  contributes to both proliferation and motility of malignant PCa cells and is successfully inhibitable by RNAi. Therefore, EF-1 $\alpha$  appears to be a potential target for antitumor therapeutic strategies, perhaps using an RNAi-based approach alone or in combination with pharmacological strategies. For further studies, we intend to provide insights into the significance of EF-1 $\alpha$  inhibition for the treatment of PCa using *in vivo* mouse models of PCa with specific EF-1 $\alpha$  inhibitors.

#### ACKNOWLEDGMENTS

This work was supported by grants from the Natural Science Foundation of Guangdong Province (04003650), the Key Programs of health bureau of Guangzhou city (2007-Zdi-05), National High Technology Research and Development Project of China (2006AA02A245; 2007AA022001), and National Natural Science Foundation of China (30872960).

#### DISCLOSURE

The authors declare that they have no competing interests as defined by *Molecular Medicine*, or other interests that might be perceived to influence the results and discussion reported in this paper.

#### REFERENCES

- Han ZD, *et al.* (2008) CD147 Expression indicates unfavourable prognosis in prostate cancer. *Pathol. Oncol. Res.* 2008, Dec 2 [Epub ahead of print].
- Han ZD, *et al.* (2009) Expression and clinical significance of CD147 in genitourinary carcinomas. *J. Surg. Res.* 10:1–8.
- Nelson WC, De Marzo AM, Isaacs WB. (2003) Prostate cancer. *N. Engl. J. Med.* 349:366–81.
- Graff JR, *et al.* (2001) Integrin-linked kinase expression increases with prostate tumor grade. *Clin Cancer Res.* 7:1987–91.
- Liao J, Schneider A, Datta NS, McCauley LK. (2006) Extracellular calcium as a candidate mediator of prostate cancer skeletal metastasis. *Cancer Res.* 66:9065–73.
- Wang J, *et al.* (2006) Increased expression of the metastasis-associated gene Ehm2 in prostate cancer. *Prostate.* 66:1641–52.
- Demma M, Warren V, Hock R, Dharmawardhane S, Condeelis J. (1990) Isolation of an abundant 50,000-Dalton actin filament bundling protein from Dictyostelium amoebae. *J. Biol. Chem.* 265:2286–91.
- Yang W, Burkhar W, Cavallius J, Merrick WC, Boss WF. (1993) Purification and characterization of a phosphatidylinositol-4-kinase activator in carrot cells. *J. Biol. Chem.* 268:393–8.
- Edmonds BT, Murray J, Condeelis J. (1995) pH regulation of the F-actin binding properties of Dictyostelium elongation factor-1a. *J. Biol. Chem.* 270:15222–30.
- Miyazaki H, *et al.* (2006) Growth factor-sensitive molecular targets identified in primary and metastatic head and neck squamous cell carcinoma using microarray analysis. *Oral Oncol.* 42:240–56.
- Wang B, Hendricks DT, Wamunyokoli F, Parker MI. (2006) A growth-related oncogene/CXC chemokine receptor 2 autocrine loop contributes to cellular proliferation in esophageal cancer. *Cancer Res.* 66:3071–8.
- Bradford MM. (1976) A rapid and sensitive method of the quantification of microgram quantities of protein utilizing the principle of protein dye binding. *Anal. Biochem.* 72:248–54.
- Liotta LA. (2001) An attractive force in metastasis. *Nature.* 410:24–5
- Liotta LA, Kohn EC. (2001) The microenvironment of the tumour-host interface. *Nature.* 411:375–9
- Liotta LA, Paweletz CP. (2002) Invasion and Metastasis. In: *The Cancer Handbook*. Alison M (editor-in-chief). Vol. 1. Nature Publishing Group, London, pp. 863–72.
- Liotta LA, Stetler-Stevenson WG. (1991) Tumor invasion and metastasis: an imbalance of positive and negative regulation. *Cancer Res.* 51:5054–9.
- Carroll SB, Stollar BD. (1983) Antibodies to calf thymus RNA polymerase II from egg yolks of immunized hens. *J. Biol. Chem.* 258:24–6.
- Dever TE, Costello CE, Owens CL, Rosenberry TL, Merrick WC. (1989) Location of seven post-translational modifications in rabbit elongation factor 1a including dimethyllysine, trimethyllysine and glycerylphosphorylethanolamine. *J. Biol. Chem.* 264:20518–25.
- Devreotes PN, Zigmond SH. (1988) Chemotaxis in eukaryotic cells: a focus on leukocytes and Dictyostelium. *Annu. Rev. Cell Biol.* 4:649–86.

20. Opdenakker G, *et al.* (1987) Human elongation factor 1 alpha: a polymorphic and conserved multigene family with multiple chromosomal localizations. *Hum. Genet.* 75:339–44.
21. Condeelis J. (1995) Elongation factor 1 alpha, translation and the cytoskeleton. *Trends Biochem. Sci.* 20:169–70.
22. Negrutskii BS, Deutscher MP. (1991) Channeling of aminoacyl-tRNA for protein synthesis in vivo. *Proc. Natl. Acad. Sci. U. S. A.* 88:4991–5.
23. Bassell GJ, Powers CM, Taneja KL, Singer RH. (1994) Single mRNAs visualized by ultrastructural in situ hybridization are principally localized at actin filament intersections in fibroblasts. *J. Cell Biol.* 126:863–76.
24. Dharmawardhane S, Demma M, Yang F, Condeelis J. (1991) Compartmentalization and actin binding properties of ABP-50: the elongation factor-1 alpha of Dictyostelium. *Cell Motil. Cytoskeleton.* 20:279–88.
25. Mohler JL, *et al.* (2002) Identification of differentially expressed genes associated with androgen-independent growth of prostate cancer. *Prostate.* 51:247–55.
26. Hannon GJ. (2002) RNA interference. *Nature.* 418:244–51.
27. Fire A, *et al.* (1998) Potent and specific genetic interference by double-stranded RNA in *Caenorhabditis elegans*. *Nature.* 391:806–811.
28. Cogoni C, Macino G. (1997) Isolation of quelling-defective (qde) mutants impaired in posttranscriptional transgene-induced gene silencing in *Neurospora crassa*. *Proc. Natl. Acad. Sci. U. S. A.* 94:10233–8.
29. Tijsterman M, Ketting RF, Okihara KL, Sijen T, Plasterk RH. (2002) RNA helicase MUT-14-dependent gene silencing triggered in *C. elegans* by short antisense RNAs. *Science.* 295:694–7.
30. Wu-Scharf D, Jeong BR, Zhang C. (2000) Transgene and transposon silencing in *Chlamydomonas reinhardtii* by a DEAH-box RNA helicase. *Science.* 290:1159–62.
31. Elbashir SM, *et al.* (2001) Duplexes of 21-nucleotide RNAs mediate RNA interference in cultured mammalian cells. *Nature.* 411:494–8.
32. Bernstein E. (2001) Role for a bidentate ribonuclease in the initiation step of RNA interference. *Nature.* 4:295–6.